

The effect of V_2O_5 on the sinterability and physical properties of Bi_2O_3 -NiO- Nb_2O_5 and Bi_2O_3 -ZnO- Nb_2O_5 temperature-stable dielectrics

KYEONG AE YEE*, KYOUNG RAN HAN, HYO TAE KIM
 P. O. Box 131 CheongRyang, Ceramics Div. KIST, 130-650, Seoul, Korea
 E-mail: kayee@kistmail.kist.re.kr

The sintering temperature of the bismuth-based temperature-stable dielectrics (BNN-BZN) is reduced down to 850 °C with 1.0 wt % of V_2O_5 , which is the lowest to our knowledge. The effect of dopant is studied in detail. The V_2O_5 seems to provide an eutectic melt below the sintering temperature to increase the sinterability. A composite character was observed with 1.0 wt % of V_2O_5 doping, while a new solid-solution phase was found without or fewer amounts of additive. Nevertheless, the obtained physical property of the sample with 1.0 wt % of V_2O_5 is promising. Following combination of physical properties is obtained consistently without any quenching procedure; dielectric constant >95, $Q \sim 2000$, T.C. = -8.6 ppm (30–100 °C), and specific resistivity = $10^{12} \Omega \text{ cm}$ © 1999 Kluwer Academic Publishers

1. Introduction

Multibillion dollars are consumed for the R&D and the production of the ceramic dielectrics every year. Much effort is endeavored on the reducing this cost, but the fundamental remedy involves substituting the noble metal used in inner electrodes with the less expensive metal like silver. The bismuth-based dielectric ceramics is worthwhile to study in this regard because they are well known low temperature firing materials. Thus, they have been studied extensively such as the piezoelectric materials, multilayer ceramic capacitors, and microwave dielectrics [1].

The BNN (Bi_2O_3 -NiO- Nb_2O_5)-BZN (Bi_2O_3 -ZnO- Nb_2O_5) studied by Ling *et al.* initially [2] is one of the promising temperature-stable dielectric materials. The reported dielectric constant and temperature coefficient (T.C.) of this system are quite comparable to the commercial materials [3, 4] as shown in Table I. Furthermore the sintering temperature is 920 °C [2] which is slightly below the melting point of Ag, 960.5 °C, while the higher temperature above 1250 °C is required for the most of commercial ones in Table I. Later Liu *et al.* [5] confirmed the some more facts on this system; (1) BNN cooperation is necessary to lower the sintering temperature of BZN (1050 °C). (2) T.C. of BNN-BZN strongly depends on the composition and heating conditions. Also, quenching is usually needed in order to obtain the expected combination of dielectric constant and T.C. (3) the degradation on the dielectric properties is observed for a certain period after application.

Further lowering of the sintering temperature is attempted to ensure the usage of cheaper electrode in

this work. Hopefully this may retard the reaction between the silver electrode and dielectrics, if exists. One finds that the addition of 0.05 wt % of V_2O_5 with 0.043 wt % of CuO improves the sinterability of the bismuth-based microwave dielectrics in the literature [6]. Neither reason for enhancing the property or their influence on the microstructure is provided in their work, however. We were able to reduce the sintering temperature of BNN ($Bi_3(Ni_2Nb)O_9$)-BZN ($Bi_2(ZnNb_{2(1+\delta)y}O_{3+6y+5\delta y})$) system down to 850 °C. The detailed study is attempted for the effect of V_2O_5 on the sintering behavior and physical properties of the studied systems for further improvement. The fixed composition of BNN with different niobium contents for BZN is studied in this work: $y = 0.8$; $\delta = 0.0113, 0.0125, 0.0250$.

2. Experimental

For BNN($Bi_3(Ni_2Nb)O_9$) synthesis, 0.15 mole of Bi_2O_3 (mol. wt. = 465.96, S.P.C. GR reagent, Shinyo Pure Chemicals Co. 99.5%), 0.19 mole of NiO (mol. wt. = 74.69, GR reagent, Aldrich Chemical Co., 99.0%), 0.05 mole of Nb_2O_5 (mol. wt. = 265.81, GR reagent, Aldrich Chemical Co., 99.9%) are ball-milled in acetone with ZrO_2 balls for 24 hours, then 0.01 mole of $Ni(NO_3)_2 \cdot 6H_2O$ (mol. wt. = 290.81, EP reagent, Shinyo Pure Chemicals Co. 97.0%) was added to the slurry and milled for two more hours. After evaporating the solvent by rotary evaporator and drying in the oven, the powder was calcined at 700 °C for an hour.

For BZN($Bi_2(Zn(Nb_{2(1+\delta)y}O_{3+6y+5\delta y})$) synthesis, stoichiometric amount of Bi_2O_3 , Nb_2O_5 and 95 mol %

* Author to whom all correspondence should be addressed.

TABLE I Dielectric constants and temperature coefficients of the commercially available dielectrics compared to those of BNN-BZN

Materials	Dielectric constant	Temperature coefficient (T.C. ppm/°C)
TiO ₂	100	-1000
MgTiO ₄ , MgTi ₂ O ₅	12-20	100-750
CaTiO ₃ , CaSiTiO ₅ [3]	80	1640
La ₂ Ti ₂ O ₇ , La ₂ Sn ₂ O ₇ [4]	12-40	50-600
Bi ₃ (Ni ₂ Nb)O ₉ ,	70-165	500
Bi ₂ (Nb ₂ Zn)O ₉		

of stoichiometric ZnO (mol. wt. = 81.37, GR reagent, Aldrich Chemical Co., 99.9%) are subjected to ball-milling in acetone for 24 hours. Then 5 mol % of Zn(NO₃)₂ · 6H₂O (mol. wt. = 290.81, EP reagent, Shinyo Pure Chemicals Co. 97%) is added to the slurry and milled for two more hours. After evaporating and drying the solvent, the powder was calcined 950 °C for two hours.

For BNN-BZN phase, a mixture of calcined 26.5 wt % of BNN and 73.5 wt % of BZN is ball-milled in 2-propanol for 24 hours. The dried powder is calcined at 800 °C for 2 hours.

Doping of BNN-BZN with several concentrations of V₂O₅ was performed by mechanical mixing in H₂O for 24 h, using propylene bottles with zirconia balls. After drying, grinding, sieving through 200 mesh, powders were isostatically pressed into a pellet with 2000 psi. The linear shrinkage was measured with dilatometer (NETZSCH, Model 402E) up to 1000 °C using a constant heating rate of 10 °C/min. The microstructure of the sintered pellet was characterized by the Electron Probe Micro Analysis (EPMA) and the densities were measured by the geometric method. The phases are determined by X-ray diffraction diffractometer (Phillips, PW 1800) using CuK_α radiation (1.5405Å) and a graphite monochromator at 40 kV, 30 mA with 3°/min of scanning speed. The dielectric constant and loss factor are measured for the polished pellet of diameter to thickness ratio, ~0.2, at 1 MHz with network analyzer (Hewlett Packard, HP8510C).

3. Results and discussion

In Fig. 1A, the phase development of BNN with varying the calcination temperature is monitored by XRD. BiDyO₃ (JCPDS#27-1040) phase has been synthesized after firing at 800 °C for an hour. BZN ($y = 0.8; \delta = 0.0125$) (Nd₂Zr₂O₇, JSPDS# 22-1189) phase development is also shown in Fig. 1B. The synthesis of the cubic pyrochlore phase is completed after two hours of firing at 950 °C. These calcination temperatures are much lower [7] than those for the mixed oxide method, with which BNN is calcined at 1050 °C/4 h and BZN at 1125 °C/4 h. This may be explained from that the nitrate reactant changes milling media to acidic to dissolve other oxides better as in Equation 1.

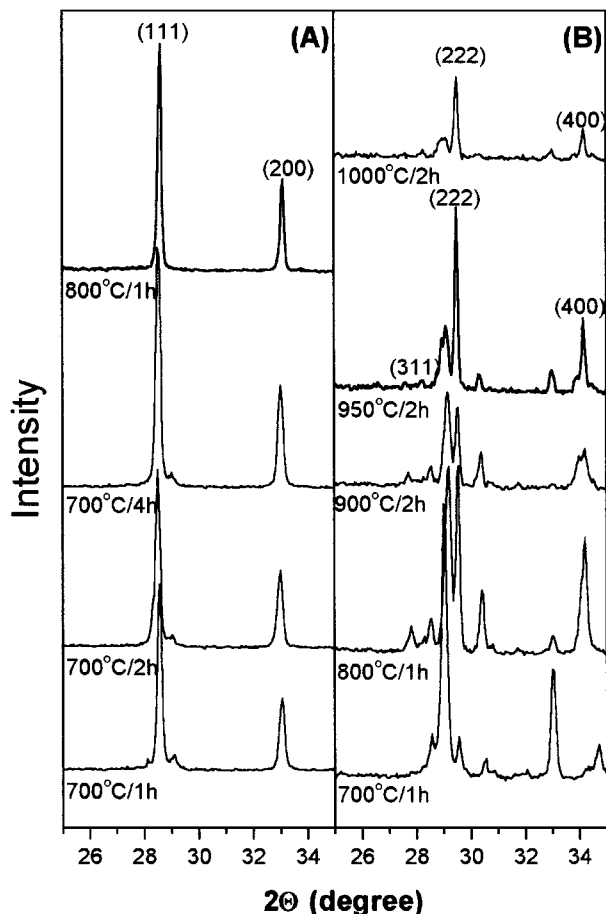
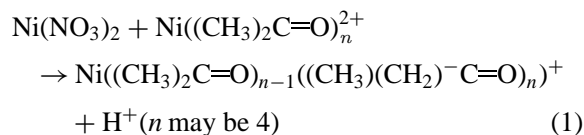


Figure 1 The phase developments of BNN (A) and BZN ($y = 0.8; \delta = 0.0125$) (B) are monitored by XRD with varying the calcination temperature.

In Fig. 2, XRD patterns for the phases calcined at 800 °C/2 h (Fig. 2A) and sintered at 920 °C/2 h (Fig. 2B) of the mixed 26.5 wt % of BNN-73.5 wt % of BZN ($y = 0.8; \delta = 0.0125$) are compared with that of the raw mixture before calcination with dotted lines in Fig. 2A. The most intense peaks of BZN(222) and BNN(111) are disappeared, while new peak appeared at 29.3°. Thus BNN-BZN mixed phase after firing does have neither BNN nor BZN crystal structure any more but may be forming a solid solution as pointed out by the previous authors [2, 5].

Furthermore, differential scanning calorimetry (DSC) data in Fig. 3 show that this sort of reaction begins below 800 °C. The broad irreversible exothermic peak at about 850 °C reveals that the more stable phase is formed above this temperature. Fig. 3A shows the thermal reactions of BNN and BZN phases prepared by the conventional mixed oxide method and Fig. 3B the modified method in which the nitrates are replaced for the oxides in part. A very similar trend is seen in both figures except for the more intense peak in Fig. 3B. This indicates the efficiency of the latter method. Since no more prominent feature is observed below this peak, the composite character may be expected for the sample fired below 700 °C.

Fig. 4 shows the XRD patterns for the BNN-BZN pellets prepared with different concentrations of V₂O₅, in which the optimal sintering temperatures are indicated. The XRD patterns for BNN (Fig. 4A) and

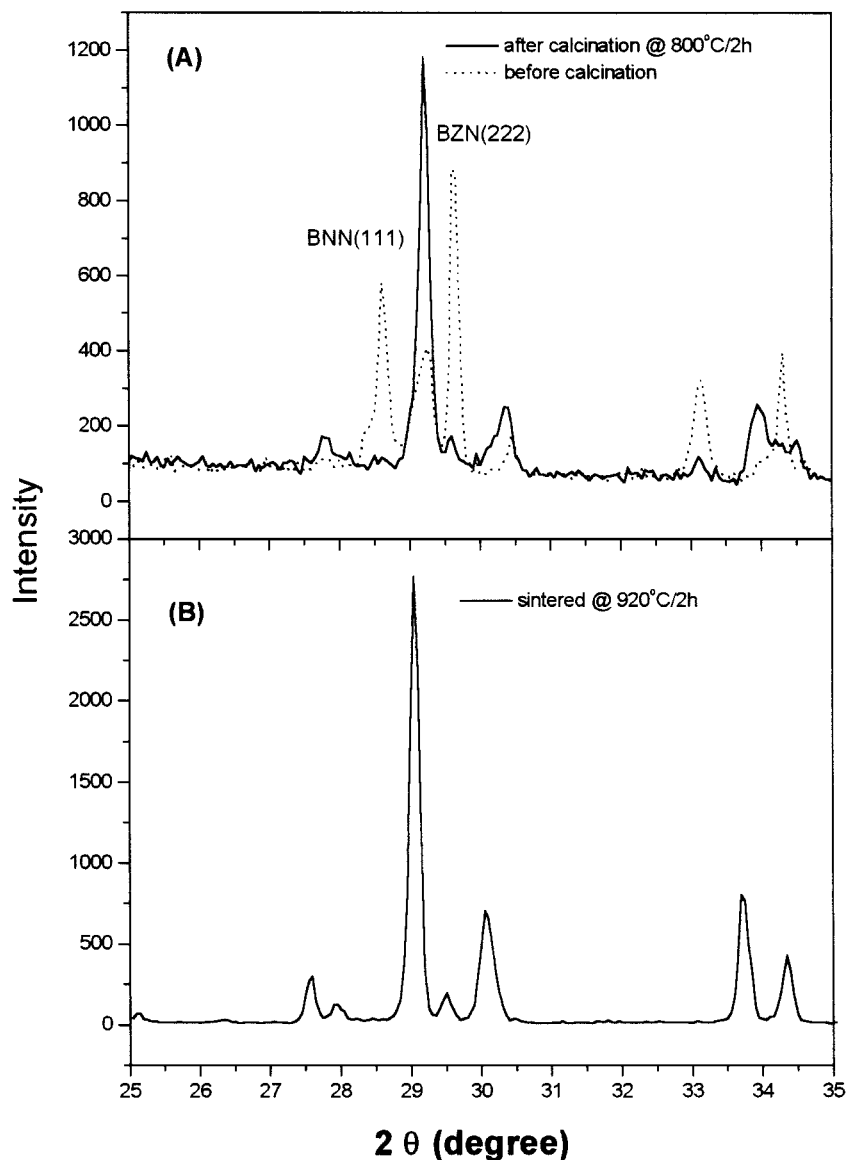


Figure 2 The XRD patterns for the mixed 26.5 wt % of BNN, 73.5 wt % BZN ($y = 0.8$; $\delta = 0.0125$). The sample calcined at $800^\circ\text{C}/2\text{h}$ with dotted lines and sintered at $920^\circ\text{C}/2\text{h}$ with solid lines in (A) are compared with raw oxides from ball-milled mixtures in (B).

BZN (Fig. 4B) are also shown for comparison. For the 0.1 wt % of V_2O_5 addition in Fig. 4C, no noticeable difference is found compared to that sintered with no dopant in Fig. 2B. However, a rather interesting feature is observed for the 1.0 wt % of V_2O_5 doped sample in Fig. 4D. While one finds a peak at 29.3° which is characteristic for the new solid solution phase, BNN(111) and BZN(222) peaks are appeared again. The two peaks at 37.3° and 43.2° are due to unreacted NiO. These peaks are also seen for the sintered pellet with 5.0 wt % of V_2O_5 concentration in Fig. 4E. No shoulder peak at 30.3° is observed in this sample that may be due to the oxygen content as pointed out in the previous report [2]. The minor phases seem not appear in the XRD pattern until 5.0 wt % of V_2O_5 is added.

The dilatometric analysis is carried out to show the effect of the V_2O_5 . In Fig. 5, the linear shrinkage rates as a function of temperature ($d(dl/l_0)/dt$) up to 965°C for a studied system with different dopant concentrations are shown. The dashed lines are for pure BNN-BZN ($y = 0.8$; $\delta = 0.0125$) sample and the dotted lines for 1.0 wt % and the solid lines for 5.0 wt % of V_2O_5 added

samples, respectively. This indicates that V_2O_5 promotes the densification of BNN-BZN very effectively.

Considering both sintering temperatures and XRD patterns, only 1.0 wt % of V_2O_5 doped BNN-BZN pellets with different niobium compositions are subjected for the following experiments. Even though 5.0 wt % of V_2O_5 added samples show better densification behavior, they are excluded out for further treatment because oxygen content is crucial to the T.C. value. In order to investigate the effect of V_2O_5 on the densification mechanism of a studied system, DSC analysis is also carried out (Fig. 6). The melting point of V_2O_5 is low as 690°C , thus the transient liquid phase may be seen before sintering temperature. DSC data of 1.0 wt % of V_2O_5 doped BNN-BZN sample is compared to that for no dopant in Fig. 3 does show sharp endothermic reactions related to the liquid-phase formation to improve the sinterability. The subsequent cooling was also carried out after a heating to observe a solidification behavior of the liquid phase. However, no clear mirror peak is observed upon cooling that indicates the existence of eutectic melting of the constituent oxides. This is

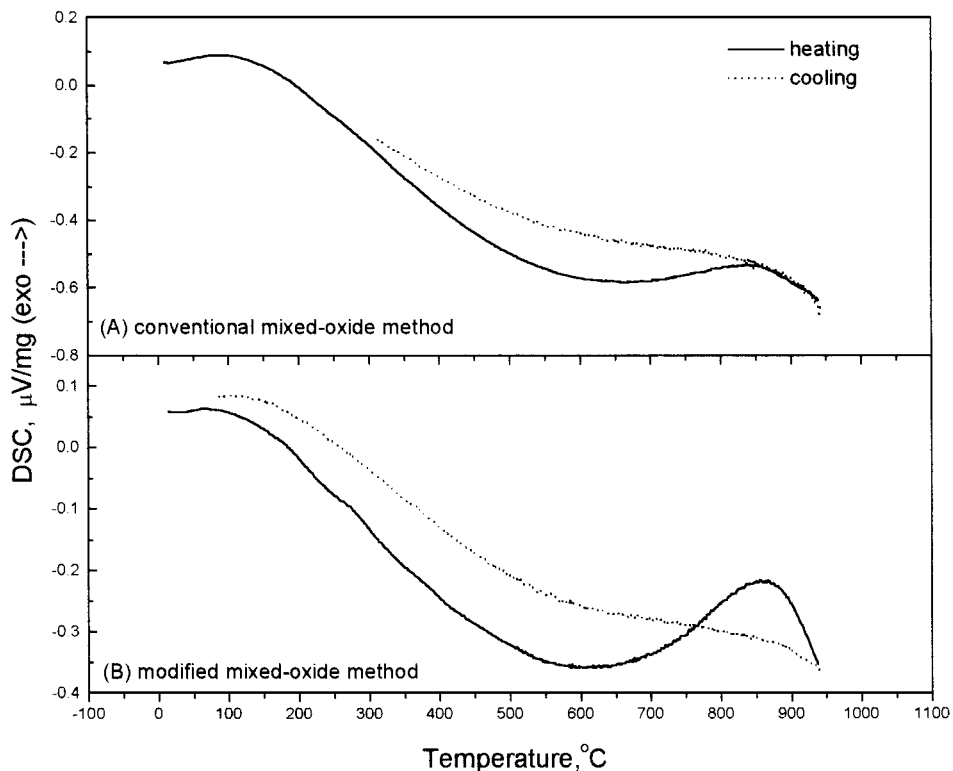


Figure 3 The thermal reactions of BNN and BZN mixtures with DSC analysis are shown for the conventional mixed oxide method in (A) and the modified one in (B), where nitrate is substituted for the constituent oxide partly. The reaction with heating condition is represented with the solid line and that with cooling with the dotted line.

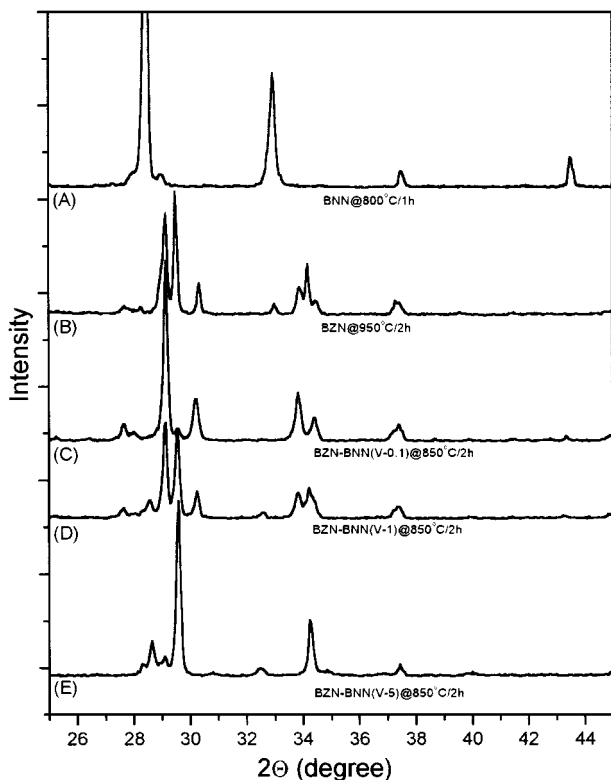


Figure 4 The XRD patterns for the BNN-BZN pellets prepared with different concentrations of V_2O_5 : (A) BNN, (B) BZN, (C) 0.1 wt % of V_2O_5 , (D) 1.0 wt % of V_2O_5 , (E) 5.0 wt % of V_2O_5 .

also evidenced by the coincident temperature at which the linear shrinkage starts for both 1.0 and 5.0 wt % of V_2O_5 doping (Fig. 5). Both heating and cooling rate are $10^\circ\text{C}/\text{min}$.

The back scattered Image obtained by Electron Probe Micro-Analyzer (EPMA) in Fig. 7 for the 1.0 wt % of V_2O_5 doped BNN-BZN ($y = 0.8$; $\delta = 0.0125$) further confirms some features found above such as liquid-phase formation and the composite features as seen in XRD pattern. Clearly, liquidus form is the white phase in the image. However, there exist three more distinguished phases beside liquidus phase; black, dark gray, and light gray. If the solubility constraint associated with the ionic radii is considered, the stoichiometry of the observed phases by EPMA is understood (Table II). Zinc (0.88 \AA) and nickel (0.83 \AA) as well as vanadium (0.68 \AA) all substitute for the niobium site (0.78 \AA) [8], then light gray phase is most likely BZN with 2 : 2 : 7 cubic pyrochlore phase. Dark gray phase is close to 3 : 3 : 9 BiDyO₃ phase, but a lot of nickel is lost. Here, the oxygen contents are calculated by the principle of electrical neutrality, which requires the total positive charges of the metal cations equal to the total negative charges of the oxides.

From the EPMA data, why BNN and BZN phases are appeared as composites for this sample in the XRD pattern (Fig. 4D) that is understood. Cation substitutions seem to result more intense peaks for both BZN and

TABLE II EPMA report for the BNN-BZN phase with 1.0 wt % V_2O_5

Phase identified	Composition
Black	$\text{Bi}_{1.28}(\text{Nb}_{0.87}\text{Ni}_{7.89}\text{Zn}_{2.87})\text{O}_{14.86}$
Liquid	$\text{Bi}_{4.20}(\text{Nb}_{0.57}\text{V}_{0.86}\text{Zn}_{0.28})\text{O}_{10.16}$
Dark gray	$\text{Bi}_{3.29}(\text{Nb}_{2.47}\text{Ni}_{0.53}\text{Zn}_{0.75})\text{O}_{12.39}$
Light gray	$\text{Bi}_{3.47}(\text{Nb}_{2.15}\text{Zn}_{0.99})\text{O}_{11.57}$

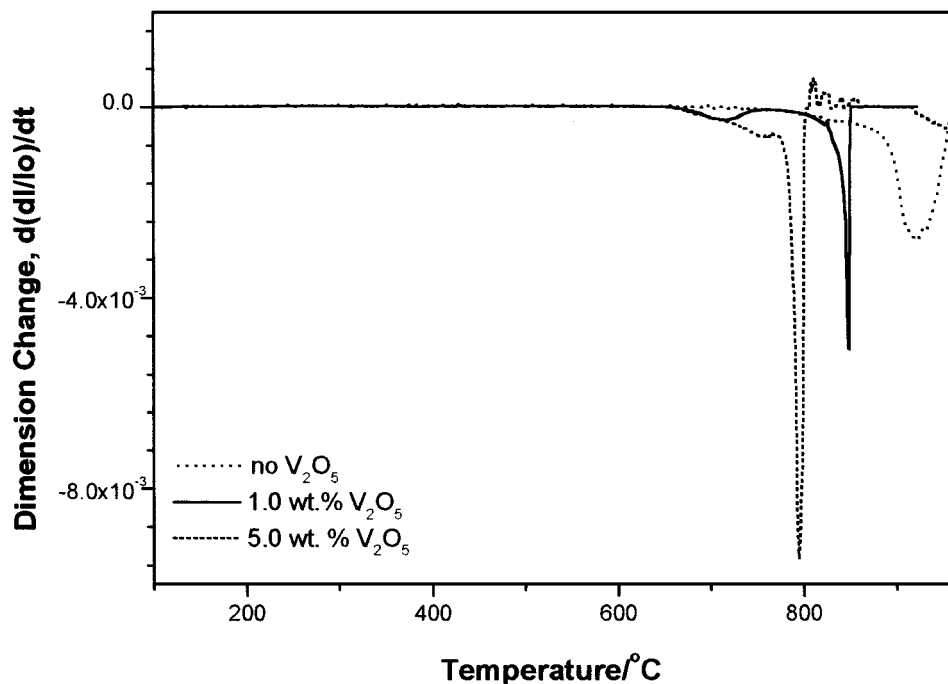


Figure 5 The effect of V_2O_5 is seen with the dilatometric analysis. The dashed lines are for pure BNN-BZN ($y = 0.8$; $d = 0.0125$) sample and the dotted lines for 1.0 wt % and the solid lines for 5.0 wt % of V_2O_5 added samples, respectively.

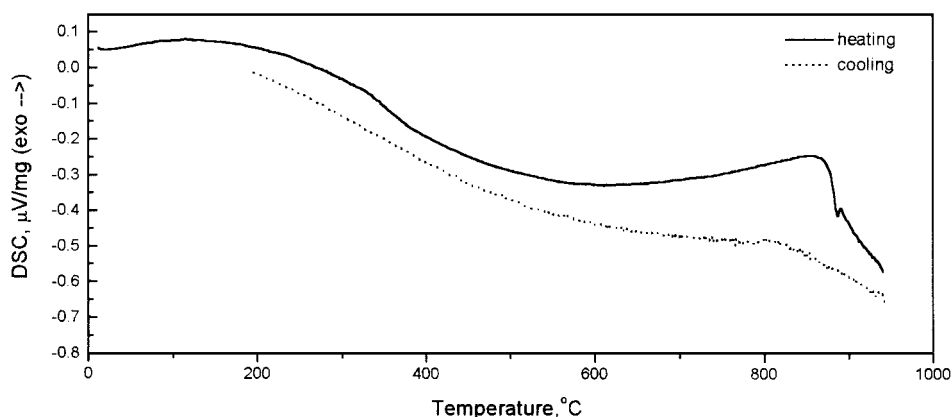


Figure 6 The thermal reaction of the BNN-BZN phases with DSC analysis is shown. The heating curve show sharp endothermic peak. The reaction with heating condition is represented with the solid line and that with cooling with the dotted line.

BNN phases. However, nickel rich black and white liquidus phase are not identified in the XRD pattern. XRD is not usually susceptible to identify the liquid/glassy phase or minor phases exist. However, the composition obtained for white phase is close to the $Bi_4M_2O_{11}$ ($M = V, Nb, Zn$) phase.

The dielectric properties for the samples of three components with 1.0 wt % of V_2O_5 added are shown in Table III. The pellets are sintered at 850 °C for two hours with the same rate. The density for the pellets

sintered at this condition is slightly higher or equal to the reported values [2]. Even though XRD pattern of 1.0 wt % V_2O_5 shows a bit different feature from that of no or low V_2O_5 added sample, a similar trend with previous report for the dielectric property is observed [2]. For example, dielectric permittivity increases with the more niobium content, and the T.C.C. also depends on the compositions. The dielectric permittivity for the samples with V_2O_5 gets slightly higher and Q lower than the literature values for the same

TABLE III Physical properties of the BNN-BZN samples sintered at 850 °C/2 h with 1.0 wt % of V_2O_5

	Sintered density (g/cm^3)	ϵ_r @1 MHz	Q@1 MHz	I.R. (Ωcm)	T.C. (ppm)
BNN-BZN ($y = 0.8$; $\delta = 0.0113$)	7.46	97.8	1633	$2.13 \cdot 10^{12}$	-8.6 (30.2–100.4 °C)
BNN-BZN ($y = 0.8$; $\delta = 0.0125$)	7.23	99.0	1636	$3.19 \cdot 10^{12}$	-24.3 (40.2–101.3 °C)
BNN-BZN ($y = 0.8$; $\delta = 0.0250$)	7.17	104.0	1935	$1.20 \cdot 10^{12}$	-128.4 (60.6–101.2 °C)

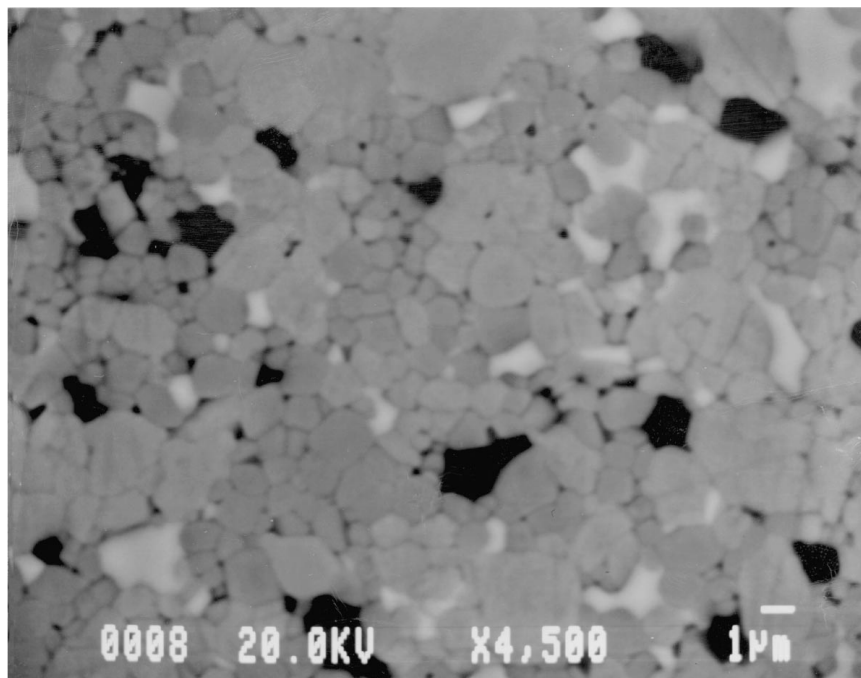


Figure 7 The back-scattered image obtained by Electron Probe Micro Analyzer (EPMA) is shown. The four phases are distinguished.

components with no dopants. The white phase in the EMPA image is suspected to increase the dielectric permittivity, since much of the bismuth niobium oxides are known as ferroelectrics [9]. Also the black phase might be responsible to increase the inductance due to high content of nickel oxide, which results lower Q factor and the resistivity than the literature values [2]. Even though it is not shown in the Table III, BNN-BZN ($y = 0.8$; $\delta = 0.0125$) with 0.1 wt % of V_2O_5 sintered at $880^\circ C/2$ h. also shows dielectric constant 78 and Q factor ~ 3000 . However, T.C. is very high.

4. Conclusions

1. Sintering Temperature of BNN-BZN system was reduced to $850^\circ C/2$ h with 1.0 wt % of V_2O_5 . Phase segregation occurred partly but the resulted physical properties are promising for the application; $Q(@1$ MHz) ~ 2000 ; $r \sim >97$; T.C. ($30-100^\circ C$) = 8.6 p.p.m. Furthermore no quenching procedure is required to get the obtained combination of properties.

2. The effect of V_2O_5 was probed by the dilatometric analysis. The DSC and EPMA show that the existence of eutectic liquid phase to improve the sinterability.

3. When 1.0 wt % of V_2O_5 is introduced, substituted BNN and BZN phases are identified with much intensified peaks by XRD. This is, also, proved by the EPMA composition analysis.

4. If the sample is prepared with the planetary milling, a sintering temperature of BNN-BZN was reduced down to $775^\circ C/2$ h. ϵ_r is improved up to 125, while Q decreases down to 1290.

References

1. T. R. SHROUT and J. P. DOUGHERTY, in "Ceramic Dielectrics; Composition, Processing & Properties in Ceramic Transactions," Vol. 8, edited by H. C. LING and M. F. YAN (The Amer. Cer. Soc. Inc., Westerville, 1990) p. 3.
2. C. H. LING, M. F. YAN and W. W. RHODES, *J. Mater. Res.* **5** (1990) 1752; M. F. YAN, C. H. LING and W. W. RHODES, *J. Amer. Cer. Soc.* **73** (1990) 1106.
3. T. M. HERBERT, "Ceramic Dielectrics and Capacitors," (Gordon and Breach Science Publishers, New York, 1985) p. 115.
4. J. TAKAHASHI and K. KAGEYAMA, in "Ceramic Transactions," Vol. 8, edited by H. C. LING and M. F. YAN (The Amer. Cer. Soc. Inc., Westerville, 1990) p. 333.
5. D. LIU, Y. LIU, S.-Q. HUANG and X. YAO, *J. Amer. Cer. Soc.* **76** (1993) 2129.
6. H. KAGATA, T. INOUE, J. KATO and I. KAKAYAMA, *Jpn. J. Appl. Phys.* **31** (1992) 3152.
7. K. R. HAN and S. J. KIM, *J. Amer. Cer. Soc.* to be published.
8. J. E. HUGHEEY, "Inorganic Chemistry," 3rd ed. (Harper & Row, New York, 1983) p. 74.
9. B. AURIVILLIUS, *Arkiv. Kemi* **1** (1949) 463; **1** (1949) 499; **2** (1950) 519.

Received 22 October
and accepted 18 November 1998